Real Time Fault Detection in Photovoltaic Cells by Cameras on Drones

Alessandro Arenella[2], Antonio Greco[1,2], Alessia Saggese[1,2(✉)], and Mario Vento[1,2]

[1] Department of Information Engineering, Electrical Engineering and Applied Mathematics (DIEM), University of Salerno, Fisciano, Italy
{agreco,asaggese,mvento}@unisa.it
[2] A.I. Tech s.r.l., 83100 Avellino, AV, Italy
arenella@aitech.vision
http://www.aitech.vision

Abstract. Hot spots are among the defects of photovoltaic panels which may cause the most destructive effects. In this paper we propose a method able to automatically detect the hot spots in photovoltaic panels by analyzing the sequence of thermal images acquired by a camera mounted on board of a drone flighting over the plant. The main novelty of the proposed approach lies in the fact that color based information, typically adopted in the literature, are combined with model based one, so as to strongly reduce the number of detected false positive. The experimentation, both in terms of accuracy and processing time, confirms the effectiveness and the efficiency of the proposed approach.

Keywords: Photovoltaic systems · Hot spot detection · Drones

1 Introduction

In the last decade we have assisted to a growing interest towards renewable energy, with particular reference to photovoltaic (PV) plants [12]. The large amount of PV plants to be monitored has led to an increasing interest of the scientific community towards those solutions able to monitor automatically, or at least semi automatically, the performance of the panels of each plant so as to detect potential faults. One of the main defects of the PV panels are the so called *hot spots* [10], corresponding to those areas in PV panels characterized by the higher temperature: indeed, in cases a cell in a panel is affected by this kind of fault, it starts dissipating power in the form of heat instead of producing electrical power [11]. This power dissipation occurring in a so small area results in a local overheating, namely the hot spot, which may cause very destructive effects: cell or glass cracking, sintering, or excessive degradation of the solar cell and thus of the related PV panel.

F. Karray et al. (Eds.): ICIAR 2017, LNCS 10317, pp. 617–625, 2017.
DOI: 10.1007/978-3-319-59876-5_68

In order to automatically detect hot spots, images acquired by thermal cameras have been widely used [2]: the main reason is that this technique is contactless and not invasive, thus it can be performed during the normal life cycle of PV systems without requiring its shut down. There are two types of thermal cameras that are typically adopted, namely radiometric and non radiometric ones (typically simply referred to as thermal cameras). The former enables the measurement of the absolute temperature, so that the intensity level of each pixel in the image corresponds to a temperature [5,9]. Of course, this kind of information may strongly simplify the analysis of the images: indeed, detecting a hot spot could be simply performed by identifying the pixels in the images with the highest temperature (above a given threshold). However, this approach is only very rarely used due to the high cost of the radiometric device. Furthermore, the accuracy in the measurement of the temperature by radiometric cameras is strongly dependent on several environmental factors (i.e. the humidity, the atmospheric temperature and the distance from the PV panels), thus a preliminary and continuous calibration of the camera is required [8]. As evident, the device calibration is a time consuming (and thus expensive) operation, especially for large PV plants, where there is a need to repeat several time this procedure.

On the other side, the usage of a (non radiometric) thermal camera does not require any calibration step. However, thermal images only provides information concerning the difference in temperature of the objects in the scene (in this case, the panels and the hotspots, as well as any other objects taken by the camera, such as trees of buildings). Hot spots pixels, due to their higher temperature, are characterized by a higher luminance than the ones of the panel to which the hot spot belongs to (but not necessarily to the other panels). Thus, the intensity distribution inside a single panel is a very powerful way for detecting possible defects. Most of the approaches proposed in the literature are based on the usage of a single thermal camera: indeed, the human operator manually takes a picture of each panel, moving the camera panel by panel. The acquired images are then automatically processed by using color based information, typically evaluating the histogram of each panel manually isolated over each image by the human operator [13]. However, this is still a time consuming operation.

In the last years, drones have been exploited for automatically acquiring the sequence of images related to the whole plant [4,12]: a drone, provided with a thermal camera, flights over the plant and acquires a video, which is manually analyzed by the human operator so as to discover the hot spots [14]. As evident, the combination between drones and thermal cameras for PV monitoring is faster (and then surely less expensive) than traditional monitoring techniques based on visual inspection on site as well as any other PV hardware devices for parameters measurement [3,7]. The manual inspection of the sequence of images, also in this case, is a very time consuming operation, thus the introduction of systems able to automatically analyze the videos and detect the hot spots becomes mandatory [1,5]. To the best of our knowledge, there are not methods able to automatically process the whole video sequence acquired by flying cameras in real time using an embedded board.

In this paper we propose an accurate and efficient method for detecting hot spots in real time analyzing videos acquired by cameras mounted over flying drones. Differently from the state of the art approaches, our method combines a *color* based analysis with a *model* based one; this choice is justified by the fact that in correspondence of the panels' junctions several high temperature points can be formed, thus implying high luminance regions in that parts of the panel, which may cause for their color intensity nature a false positive. Starting from this consideration, the proposed algorithm detects the panels in the PV module by exploiting geometry and structural information of the panels, then evaluates the color of each panel, independently on the other ones. Finally, the position of the potential hot spot is analyzed with respect to its panel so as to filter out those hot spots close to the junctions. The accuracy of the proposed approach is not paid in terms of execution time. Indeed, another contribution of this paper lies in the fact that the algorithm has been designed for running over System on a chip (SoC) architectures: the video is not acquired and sent to an external server, but instead is processed directly on board of the SoC mounted on the drone, so that only the position of the hot spots (and a couple of images associated to it) is notified to the human operator driving the drone, for an immediate check.

2 The Proposed Method

The method is based on the following three steps, whose output is shown in Fig. 1: (i) during the Preprocessing step, the lines in the images (white lines in Fig. 1b) are extracted and used to align the image and to (ii) find out the panels in the modules (identified by the white rectangles in Fig. 1c). Finally, for each detected panel, the (iii) detection of the hot spots is performed (the red rectangle in Fig. 1d).

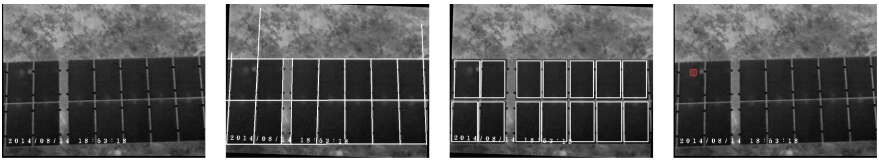

(a) Original Frame (b) Preprocessing (c) PV Detection (d) Hot spot

Fig. 1. The different steps of the proposed approach. (Color figure online)

2.1 Preprocessing

During the preprocessing step, the lines inside each image are detected by using the Hough transform (see Fig. 2a). As we can see from the figure, the mere application of this technique is not sufficient since the following problems arise: several spurious lines are detected, while only horizontal and vertical lines should be considered; for each junction, more than one line is detected; finally, several

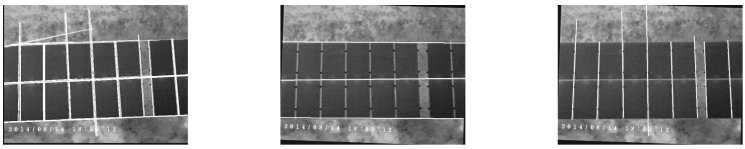

(a) Lines (b) Horizontal (c) Vertical

Fig. 2. Preprocessing step: (a) application of the Hough transform on the image; (b) horizontal and (c) vertical lines extracted by the proposed approach.

lines are longer than the corresponding panels. In order to deal with these problems, the proposed approach is based on the following steps: (i) depending on the slope of the lines, two sets are formed, namely horizontal and vertical lines. (ii) Then, the average slope $\bar{m}$ of each set is computed and each line $y = m \cdot x + n$ is evaluated; in case $|\bar{m} - m| > T$, the line is filtered out since it is considered as an error of the previous step. (iii) In order to merge all those lines corresponding to the same junction, a hierarchical clustering algorithm based on the distance between the lines is then applied. Finally, (iv) the alignment of the image is performed:

$$A = \begin{bmatrix} \cos\alpha & \sin\alpha\ (1 - \cos\alpha) \cdot x_0 - \sin\alpha \cdot y_0 \\ -\sin\alpha & \cos\alpha \sin\alpha \cdot x_0 + (1 - \cos\alpha) \cdot y_0 \end{bmatrix} \quad (1)$$

The transformation matrix A performs an elementary rotation around the z axis of an angle α, computed as the average rotational angle of the horizontal lines. This rotation is carried out with respect to the center of the image, namely (x_0, y_0). In more details, the rotated image RI is obtained starting from the original image I as follows: $RI(x, y) = I(A_{11}x + A_{12}y + A_{13}, A_{21}x + A_{22}y + A_{23})$. The lines (both horizontal and vertical) are rotated by using the same transformation matrix A, so as to avoid their re-computation after the image rotation. An example of the output of this step over the image in Fig. 1a is reported in Figs. 2b and c.

2.2 Panels Detection

During this step, all the panels contained in each image are detected by recognizing their geometric and structural properties. Indeed we start from the following assumptions: (i) a vertical line can be considered as the border of a panel (and then a *true line*) if the distance with respect to the other vertical lines is approximatively a multiple value of the panel width. (ii) The same assumption holds for horizontal lines. (iii) The whole grid has exactly four borders: two external vertical true lines and two external horizontal true lines. Thus, only the true lines respecting the above constraints are considered and the external borders of the grid are extracted. The above actions are able to only deal with false positive lines, but not with misses lines. In order to face with this problem, the proposed approach exploits structural information of the panels: indeed, missing lines, both horizontal and vertical, are added so as to make uniform the grid of panels in the image, as shown in the two examples reported in Fig. 3.

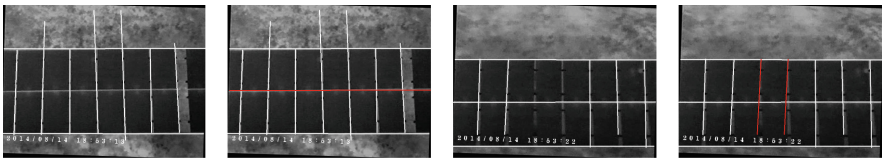

(a) True lines (b) Grid correction (c) True lines (d) Grid correction

Fig. 3. Panels detection step: (a, c) true lines in white; (b, d) red lines are added by the proposed approach so as to correct the grid. (Color figure online)

Once the lines have been corrected, the rectangles, each corresponding to a panel, are identified: the intersections between horizontal and vertical lines are considered and used as the corners of the rectangles. An example is reported in Fig. 1c. In order to be considered a *true panel*, the size of the panel should be within a range identifying the expected size of the panel, which is a priori known.

2.3 Hot Spot Detection

For each panel identified during the previous step, the algorithm verifies the presence of the hotspots, corresponding to those higher temperature areas far from the junctions of the panels. In more details, the Sobel Edge Detector is applied in each panel so as to compute the gradient, in each panel independently on the other ones. Differently from other operators, Sobel has been chosen due to its efficiency. Starting from the gradient, each cell is thresholded and the corresponding mask is computed (see Fig. 4); thus, the connected components are found and their positions are evaluated; components located on the borders are filtered, as shown in Fig. 4b.

(a) Panel (b) Mask (c) Panel (d) Mask

Fig. 4. PV panels (a, c) and the corresponding masks (b, d). The connected component in (b) is filtered thanks to the evaluation of the position based information. The red box in (d) is the hot spot detected by the system. (Color figure online)

3 Experimental Dataset

In this section we will discuss the results obtained by the proposed approach, analyzing both the accuracy and the processing time over SoC architectures.

Since there are not any datasets available in the literature for this purpose, we decided to use our own dataset. Five different videos have been acquired during real PV plant inspections by an Italian company, namely Topview s.r.l., which builds drones and provides PV inspection services. The videos have been acquired with a thermal camera mounted over a quadcopter DJI. They are representative of the different conditions this typology of algorithms could face with; indeed, they differ in terms of resolution, frame rate and length (corresponding to different dimensions of the plant). Furthermore, the cameras used for the acquisition are different (thus the optical properties of the camera), as well as the height of the drone' flight. Such properties impact on the average number of panels that can be seen in a single frame (from 8 to 30). An overview of the features of the datasets are reported in Table 1, where details concerning the orientation of the panels (V: vertical; H: horizontal), together with the direction of the movement of the drone (EW: from east to west; NS: from north to south; SN: from south to north), are also detailed. An example for each video is reported in Fig. 5.

Table 1. Description of the dataset used in our experimentations.

Video	# Frame	FPS	Resolution	Movement	# Panels	Orientation
Video 1	400	25	640×480	EW	14	V
Video 2	100	25	336×256	SN	24	H
Video 3	525	25	336×256	NS	8	H
Video 4	85	1	336×256	EW	30	H
Video 5	61	1	336×256	NS	8	H

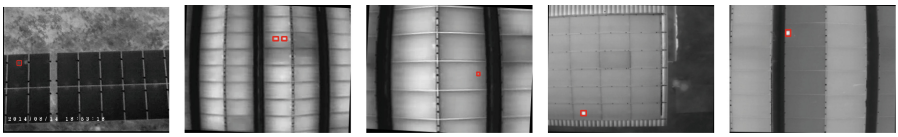

(a) Video 1 (b) Video 2 (c) Video 3 (d) Video 4 (e) Video 5

Fig. 5. Some examples of the considered dataset.

The performance of the proposed approach has been computed in terms of True Positive (TP), False Positive (FP), Precision (P), Recall (R) and F-Score (F) by using the Pascal Criterion [6]. In more details, given the bounding box T_i associated to the hotspot at the ith frame and the ground truth box, GT_i, the overlap between such boxes is evaluated. T_i can be considered a TP if it satisfies the following condition: $\frac{area(T_i \cap GT_i)}{area(T_i \cup GT_i)} \geq K$, where K has been fixed to 0.4. All the detected hotspots T_i which do not satisfy the previous equation can be considered FP. Given TP and FP, the remaining indices can be evaluated as

Table 2. Performance of the proposed approach (combining color and model based information) compared with a traditional color based approach.

Video	Proposed approach						Color based approach						Improvement
	TP	FP	FN	P	R	F	TP	FP	FN	P	R	F	
Video 1	64	87	49	0.42	0.58	**0.49**	64	931	49	0.10	0.58	0.12	308%
Video 2	179	215	19	0.45	0.90	**0.61**	178	952	20	0.16	0.90	0.27	126%
Video 3	309	295	140	0.51	0.69	**0.59**	309	547	140	0.36	0.69	0.47	25%
Video 4	25	7	7	0.78	0.78	**0.78**	25	140	7	0.15	0.78	0.25	212%
Video 5	17	12	3	0.59	0.85	**0.69**	17	31	3	0.35	0.85	0.50	38%

follows: $P = \frac{TP}{TP+FP}$, $R = \frac{TP}{TP+FN}$, $F = 2 \cdot \frac{P \cdot R}{P+R}$. The obtained results are summarized in Table 2. Since there are not publicly available datasets that consist of videos or images for this specific purpose, we compare the proposed method with the baseline approach, which only evaluates the color based information. From the table, we can note that the main difference between the two algorithms pertains the number of false positives that the proposed approach is able to filter out thanks to the introduction of the model based information. The overall improvement with respect to the baseline approach is significant, ranging from 25% up to 308%, thus confirming the effectiveness of the proposed approach.

In order to also provide a qualitative evaluation of the proposed approach, the following link[1] shows its behavior in action.

In order to verify the effectiveness of the proposed approach even from a computational point of view, we performed an analysis in terms of time required for the computation. The analysis has been conducted over a SoC Intel Joule 570X, equipped with a CPU quad core Intel Atom T5700@1,7 GHz (max 2,4 GHz) and 4 GB RAM LPDDR4. Thanks to its size, this device can be mounted directly on board of the drone, so as to allow a real time processing. The results obtained by the proposed approach, expressed in terms of frame rate, are reported in Table 3. It is worth to point out that five different values have been reported due to the different typologies of videos. We can note, for instance, that the processing

Table 3. Time analysis of the proposed approach.

Video	Preprocessing	PV detection	Hot spot detection	FPS
video 1	95.32%	0.06%	4.62%	8
video 2	96.28%	0.15%	3.57%	11
video 3	97.12%	0.12%	2.76%	18
video 4	96.46%	0.12%	3.42%	10
video 5	96.87%	0.13%	3.00%	15

[1] http://mivia.unisa.it.

of the Video 1, acquired at a 4CIF resolution, is slower than the other videos, acquired at a resolution of 1CIF.

Table 3 also reports the percentage of the time required for the elaboration of each phase (namely preprocessing, PV detection and hot spot detection). As expected, the most time consuming operation is the preprocessing step, mainly due to the Hough transform used for the extraction of the lines. However, the obtained frame rate confirms the possibility for the proposed approach to run over a SoC architecture in real time (from 8 to 18 frames per seconds), even using a full 4CIF resolution. This is an important contribution of the proposed approach, since there are not any methods available in the literature thought for running directly in real time over SoC architectures.

4 Conclusions

In this paper we proposed a method for detecting the hot spots in a PV plant by processing the images acquired by a thermal camera mounted on board of a drone. The main novelty is that a model based approach is combined with a traditional color based one so as to increase the overall reliability of the proposed method. The results, obtained over five videos acquired in real PV plants, show that our method is able to run in real time over SoC architecture, obtaining very promising results. The possibility to run over SoC architectures is another important contribution of this paper.

References

1. Aghaei, M., Grimaccia, F., Gonano, C.A., Leva, S.: Innovative automated control system for PV fields inspection and remote control. IEEE Trans. Ind. Electron. **62**(11), 7287–7296 (2015)
2. Buerhop, C., Schlegel, D., Niess, M., Vodermayer, C., Weißmann, R., Brabec, C.: Reliability of IR-imaging of PV-plants under operating conditions. Solar Energy Mater. Solar Cells **107**, 154–164 (2012)
3. Buerhop-Lutz, C., Scheuerpflug, H.: Inspecting PV-plants using aerial, drone-mounted infrared thermography system. In: 3rd Southern African Solar Energy Conference, South Africa, 11–13 May 2015 (2015)
4. Denio, H.: Aerial solar thermography and condition monitoring of photovoltaic systems. In: Photovoltaic Specialists Conference (PVSC), pp. 613–618. IEEE (2012)
5. Dotenco, S., Dalsass, M., Winkler, L., Brabec, C., Maier, A., Gallwitz, F., et al.: Automatic detection and analysis of photovoltaic modules in aerial infrared imagery. In: 2016 IEEE International Conference on WACV, pp. 1–9 (2016)
6. Everingham, M., Van Gool, L., Williams, C.K., Winn, J., Zisserman, A.: The pascal Visual Object Classes (VOC) challenge. Int. J. Comput. VIs. **88**(2), 303–338 (2010)
7. Grimaccia, F., Aghaei, M., Mussetta, M., Leva, S., Quater, P.B.: Planning for PV plant performance monitoring by means of Unmanned Aerial Systems (UAS). Int. J. Energy Environ. Eng. **6**(1), 47–54 (2015)
8. Jensen, A.M., McKee, M., Chen, Y.: Calibrating thermal imagery from an unmanned aerial system-AggieAir. In: 2013 IEEE IGARSS, pp. 542–545 (2013)

9. Kaplani, E.: Detection of degradation effects in field-aged c-Si solar cells through IR thermography and digital image processing. Int. J. Photoenergy **2012**, 11 p. (2012). Article no. 396792. doi:10.1155/2012/396792
10. Manganiello, P., Balato, M., Vitelli, M.: A survey on mismatching and aging of PV modules: the closed loop. IEEE Trans. Ind. Electron. **62**(11), 7276–7286 (2015)
11. Nguyen, D.D., Lehman, B.: Modeling and simulation of solar PV arrays under changing illumination conditions. In: 2006 IEEE Workshops on Computers in Power Electronics, pp. 295–299. IEEE (2006)
12. Quater, P.B., Grimaccia, F., Leva, S., Mussetta, M., Aghaei, M.: Light Unmanned Aerial Vehicles (UAVs) for cooperative inspection of PV plants. IEEE J. Photovoltaics **4**(4), 1107–1113 (2014)
13. Tsanakas, J., Botsaris, P.: On the detection of hot spots in operating photovoltaic arrays through thermal image analysis and a simulation model. Mater. Eval. **71**(4), 457–465 (2013)
14. Tyutyundzsshiev, N., Martínez Moreno, F., Leloux, J., Narvarte Fernández, L.: Equipment and procedures for ON-SITE testing of PV plants and BIPV. IES (2014)